

MIMO OFDM DOA Estimation Algorithm Implementation and Validation Using SDR Platform

Levon N. Grigoryan, Martin Ts. Aivazyan, and Arshak S. Babayan

Original scientific paper

Abstract—The work is devoted to research in Mobile Station (MS) positioning techniques having opportunity and perspective of using in the next generation communication networks, particularly in cellular networks. Direction of Arrival (DOA) estimation is necessary in many positioning applications and has been well studied by academy and by industry. The main contribution of this work is to design and implement a computationally light direction of arrival estimator on a Multiple Input Multiple Output (MIMO) Software Defined Radio (SDR) platform. Implemented direction of arrival estimator is tested and validated in real conditions and experimental measurements show, that the implemented algorithm can accurately estimate the directions of arrived signals. Used algorithm, estimates direction of arrivals by processing received data of 16-element two dimensional planar antenna array. The algorithm uses initial data received from channel estimators and further process it to obtain direction information. The hardware implementation has been thoroughly analyzed and experimentally validated and open source host code is available on Github.

Index Terms— Antenna arrays, Direction of arrival estimation, MIMO, Mobile communication, OFDM, Software defined radio.

I. INTRODUCTION

Future communication systems should provide not only high data transmission rate but also the global change of our understanding of wireless communications. Today, number of devices that are connected to the Internet is rapidly growing, and there is a following trend: everything will be connected to the Internet, starting from power supply systems and medical equipment, to the traffic lights, household appliances and cars (implementation and integration of IoT (Internet of Things), D2D (Device-to-Device) and M2M (Machine-to-Machine)

Manuscript received September 13, 2018; revised December 6, 2018. Date of publication January 10, 2019. The associate editor Prof. Gordan Šišul has been coordinating the review of this manuscript and approved it for publication.

This work was supported in part by ISTC JRGF (111-A-15-00001) and NI Armenia academy program.

L. N. Grigoryan, M. Ts. Aivazyan, and A. S. Babayan are with the Institute of IT and Electronics, National Polytechnic University of Armenia, Yerevan, Armenia (e-mails: levon.grigoryan.01@gmail.com, aivazyan@seua.am, arshbabayan@mail.ru).

Digital Object Identifier (DOI): 10.24138/jcomss.v15i1.618.

technologies). This opens unlimited possibilities for society, business and other fields of human activity. Growth of number of connected devices will be accompanied by the emergence of new methods of their use, that lead to new requirements for the next generation mobile networks [1]. MS precise position tracking is one of the challenges of future networks. High precision positioning information is a fundamental component of autonomous systems and location aware applications in mobile devices. Additionally it could be used by special services to detect subscriber location or by subscriber itself. The Global Navigation Satellite System (GNSS) works well outdoors, but the accuracy and robustness degrade severely in scenarios like urban canyons and indoor environments due to poor propagation conditions between satellites and user equipment [2]. In contrast, cellular and wireless networks generally have good coverage in those GNSS harsh environments. As a substitute or supplement to GNSS, radio-based positioning techniques could be good alternative.

Direction finding and positioning techniques have been applied for a long time in radar applications: they were used for air traffic control, target acquisition, position tracking systems. More recently, positioning techniques have been applied to wireless communications for mobile terminals localization. There are well-known position estimation techniques like triangulation and trilateration. In triangulation, it is necessary to estimate Direction of Arrival (DOA) angle of received signals by a set of sensors or antenna array.

Researchers proposed many approaches to DOA estimation. Some of them including beamforming, array correlation matrix, eigenanalysis, linear prediction, minimum variance, maximum likelihood, minnorm, MUSIC, root-MUSIC, and ESPRIT techniques could be found in [3]-[5].

The beamforming, minimum variance and maximum likelihood techniques are some of the first techniques investigated for DOA estimation. Due to the low resolution of beamforming, minimum variance and intensive computation in the maximum likelihood techniques, they are less popular than other techniques. On the other hand, the subspace-based methods search for directions by decomposing a matrix formed

from the received signal samples into two subspaces: noise subspace and signal subspace. Once the signal subspace has been determined, the data model parameters can then be extracted. Two widely used subspace-based techniques for DOA estimation are Multiple Signal Classification (MUSIC) and Estimation of Signal Parameters via Rotational Invariance Techniques (ESPRITs).

Beamforming technique, also called Bartlett DOA estimation technique, met requirements for low computational complexity but the ability to resolve angles is limited by the array half-power beamwidth. This is one of the limitations of the Bartlett approach to DOA estimation. In classical approach, an increase in resolution requires a larger array.

It is anticipated, that Multi User Multiple Input Multiple Output (MU-MIMO) transmission techniques due to robust properties and several key advantages over Single User Multiple Input Multiple Output (SU-MIMO) communications, will be widely used in future wireless communication networks [6]. MU-MIMO requires channel state information of all users at transmitter to properly serve the spatially multiplexed users. Several papers have addressed implementation of DOA estimation using FPGAs; examples of which are Bartlett algorithm [7], ESPRIT algorithm [8] and MUSIC algorithm [9]. This paper, on the other hand, focuses on implementation of a Bartlett algorithm on the host in MU-MIMO scenario and channel state information estimation implemented on the FPGA.

The contributions of this work are:

- 1) The host implementation of three-dimensional DOA estimation algorithms' key operations.
- 2) The National Instruments MIMO SDR prototyping platform is used to build a complete prototype of MU-MIMO DOA estimation algorithm. This prototype has produced results, which show good agreement between the experimental DOA estimates and true values.
- 3) The share of experiment open source software to facilitate reproducibility.

In the next section, we briefly discuss the basic concepts of DOA estimation algorithm under consideration and present its key mathematical operations.

II. DOA ESTIMATION BY USING CHANNEL STATE INFORMATION

A. Background

In selected model, a transmitted narrowband waveform at transmission point expressed as [10]

$$E(0, t) = s(t)e^{j\omega t} \quad (1)$$

where $s(t)$ is slowly time varying compared to the carrier $e^{j\omega t}$. Further, in the text uppercase and lowercase Greek letters are to be understood as matrices or vectors within their context.

For $|\mathbf{r}| \ll c/B$, where B is the bandwidth of $s(t)$, assuming far field conditions met and wave front is plane we can write

$$E(\mathbf{r}, t) = s(t - \mathbf{r}^T \boldsymbol{\alpha})e^{j\omega(t - \mathbf{r}^T \boldsymbol{\alpha})} \cong s(t)e^{j(\omega t - \mathbf{r}^T \mathbf{k})} \quad (2)$$

$|\mathbf{k}| = \frac{\omega}{c} = 2\pi/\lambda$ is the wavenumber, λ is the wavelength and $|\boldsymbol{\alpha}| = \frac{1}{c}$ is the slowness vector, where c is the wave propagation speed.

In general, \mathbf{k} is a vector and its direction coincides with signal propagation direction. In the xy -plane we have

$$\mathbf{k}_x = |\mathbf{k}| \cos \theta \quad (3)$$

$$\mathbf{k}_y = |\mathbf{k}| \sin \theta \quad (4)$$

where θ is a counterclockwise angle between propagation direction and x -axis.

In the model, an array element is represented as a point receiver at specific spatial coordinates and \mathbf{r}_ℓ radius vector.

For 2D case using (2) the field generated by a source at azimuthal DOA θ at array element ℓ is given by

$$E(\mathbf{r}_\ell, t) = s(t)e^{j\omega t - \mathbf{k}\mathbf{r}_\ell} = s(t)e^{j\omega t - (\mathbf{k}_x \mathbf{r}_{\ell x} + \mathbf{k}_y \mathbf{r}_{\ell y})} \quad (5)$$

also by using (3) and (4), (5) could be modified as

$$E(\mathbf{r}_\ell, t) = s(t)e^{j\omega t - k(\cos \theta \mathbf{r}_{\ell x} + \sin \theta \mathbf{r}_{\ell y})} \quad (6)$$

Assuming all array elements have flat frequency response over frequency bandwidth and directivity $g(\theta)$, its measured output will be proportional to the electromagnetic field at antenna element. Ignoring carrier term $e^{j\omega t}$ for convenience, the output of the array element at specified point will be modeled by

$$x_\ell(t) = g(\theta)e^{jk(\cos \theta \mathbf{r}_{\ell x} + \sin \theta \mathbf{r}_{\ell y})}s(t) = a_\ell(\theta)s(t) \quad (7)$$

Overall array output vector is obtained as

$$\mathbf{x}(t) = \mathbf{a}(\theta)s(t) \quad (8)$$

Assuming antenna array is a linear receiving system

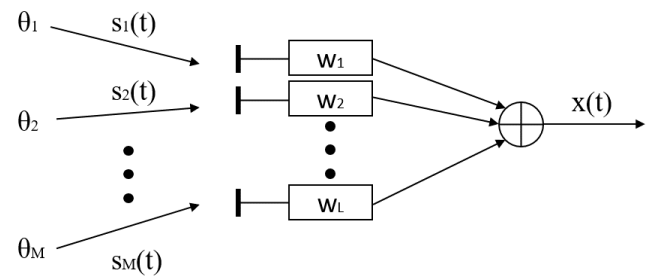


Fig. 1. Receiving system block diagram.

superposition principle is applicable. As a generalization, if M signals received by L element array from distinct DOAs $\theta_1, \theta_2, \theta_3 \dots \theta_M$ the output vector takes the form

$$\mathbf{x}(t) = \sum_{i=1}^M \mathbf{a}(\theta_i)s_i(t) \quad (9)$$

where $s_i(t)$ denote the baseband signal waveforms.

Defining a steering matrix and a vector of signal waveforms as

$$\mathbf{A}(\theta) = [\mathbf{a}(\theta_1), \mathbf{a}(\theta_2) \dots \mathbf{a}(\theta_M)] \text{ (L} \times \text{M)}$$

$$\mathbf{s}(t) = [s_1(t), s_2(t) \dots s_M(t)]^T$$

and taking into account presence of an additive noise $\mathbf{n}(t)$, (9) can be put in a more compact form

$$\mathbf{x}(t) = \mathbf{A}(\theta)\mathbf{s}(t) + \mathbf{n}(t). \quad (10).$$

B. DOA Estimation Bartlett Method

The main idea of Bartlett beamformer is to steer the antenna beam in all directions and measure the output power. Antenna beam is steered by changing weighting vector (\mathbf{w}) which acts like a spatial filter. Estimated DOA of arrived signal corresponds to a set of weights \mathbf{w} that maximizes the received signal power.

Suppose we wish to maximize output power from a certain direction (θ). Measured array output signal is defined in (10). The problem of maximizing the output power is formulated as

$$\max_{\mathbf{w}} E\{\mathbf{w}^H \mathbf{x}(t) \mathbf{x}^H(t) \mathbf{w}\} = \max_{\mathbf{w}} \mathbf{w}^H E\{\mathbf{x}(t) \mathbf{x}^H(t)\} \mathbf{w} = \max_{\mathbf{w}} E\{|\mathbf{s}(t)|^2 |\mathbf{w}^H \mathbf{a}(\theta)|^2 + \sigma^2 |\mathbf{w}|^2\}. \quad (11)$$

When carrying out the above maximization the norm of \mathbf{w} is constrained to 1 in order to obtain a non-trivial solution.

The non-trivial solution of (11) is

$$\mathbf{w}_{BF} = \frac{\mathbf{a}(\theta)}{\sqrt{\mathbf{a}^H(\theta) \mathbf{a}(\theta)}}. \quad (12)$$

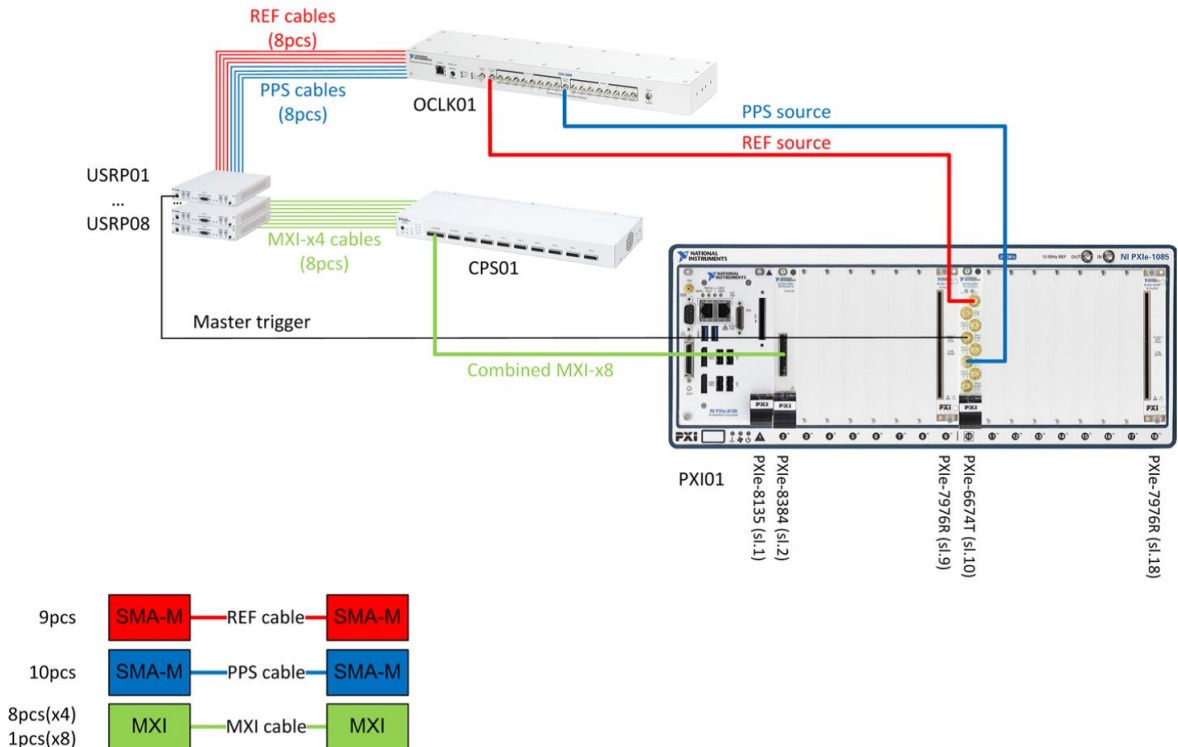


Fig. 2. BS architecture and connection diagram [11].

The final spatial spectrum is obtained by

$$\mathbf{P}_{BF}(\theta) = \mathbf{w}_{BF}^H \check{\mathbf{R}} \mathbf{w}_{BF} = \frac{\mathbf{a}^H(\theta) \check{\mathbf{R}} \mathbf{a}(\theta)}{\mathbf{a}^H(\theta) \mathbf{a}(\theta)} \quad (13)$$

where $\check{\mathbf{R}}$ is the sample covariance matrix

$$\check{\mathbf{R}} = \frac{1}{N} \sum_{i=1}^N \mathbf{x}(t) \mathbf{x}^H(t) \quad (14)$$

and N is size of finite data set.

III. HARDWARE CONFIGURATION

A. System Overview

National Instruments equips engineers and scientists with systems that accelerate productivity, innovation, and discovery. We use MIMO prototyping system provided by NI to validate developed DOA estimation algorithm and build prototype that works in real world conditions, utilizing LTE like frame structure, fully-functional PHY for bi-directional transmission, as well as basic medium access control layer elements and is ready for additional research and modifications. The main functionality of system allows [11]:

- Multi-user MIMO transmission between one BS with 16 antennas and up to 12 single antenna MSs.
- Bi-directional, OFDM-based time-division duplex (TDD) transmission using 20 MHz signal bandwidth.
- Channel reciprocity calibration for all radio units at the BS.

- Linear multi-user MIMO precoding and equalization for up to 16×12 antenna systems. Options include: Minimum mean squared error (MMSE), zero-forcing (ZF), and maximum-ratio combining (MRC). Multi-user MIMO precoding (at the BS) is channel reciprocity based.

- Automatic gain control (AGC) at the BS and MS.
- Variable modulation schemes ranging from 4-quadrature amplitude modulation (QAM) to 256-QAM.
- Support of packet-based user data transmission in DL and UL to enable data streaming applications, such as video transmission.

All listed functionality, such as modulation, over-the-air synchronization, MIMO equalization and MIMO precoding are based on real time signal processing implemented on FPGA.

The system consists of the following main components:

- One 16 antenna BS.
- One or more MSs.

B. Base Station Configuration

The BS hardware used during this work consists of 8 USRP 2953s, a PXIe-1085 chassis equipped with PXIe-8135 controller, PXIe-6674T synchronization and timing module for precise 10MHz reference clock generation and USRP's synchronization, two PXIe-7976 FPGA modules for data processing, PXIe-8384 MXI-Express module for communication with the USRP RIO devices (through the CPS-8910). The BS connection diagram is shown in Fig. 2.

Clock and synchronization signals are distributed to eight USRP subsystems through the CDA-2990 (OCLKM1). The CDA-2990 provides both clock and time synchronization by amplifying and distributing the 10 MHz reference signal (generated by the PXIe-6674T) and by amplifying and distributing the pulse per second (PPS) signal from the master USRP RIO device to the eight USRP RIO devices through matched-length cables. All RIO devices within subsystem are connected to a CPS-8910 device.

RF front ends of USRPs are through shielded RF cables connected to VERT 2450 antennas. Each USRP is connected to two antennas. All 16 antennas are mounted on a flat plane having 2D planar array geometry shown in Fig. 3.

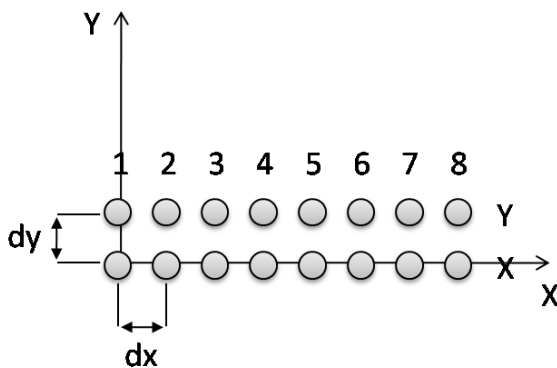


Fig. 3. Testbed antenna array configuration.

Physical distance among antennas in X direction is equal to

5cm, in Y direction to 4.5cm. The BS overall view is presented in Fig. 4.



Fig. 4. Testbed BS front view.

C. Mobile Station Configuration

A MS represents a handset or another wireless device with single input, single output (SISO) wireless capabilities. The system supports up to 12 simultaneous single antenna MSs. The single antenna MS prototype uses a USRP RIO device with an integrated GPS disciplined oscillator (GPSDO). Each USRP RIO device through a PCI Express cable is connected to a laptop. The GPSDO is important because it provides improved clock accuracy exploited by the single antenna MS implementation. It also enables GPS-based synchronization among MSs. In general, system includes multiple MSs, where each USRP RIO represents up to two single antenna MS devices. MS overall view is presented in Fig. 5.

As could be seen from Fig. 5, MS can be freely moved within



Fig. 5. Testbed MS overall view.

a room and rotated in order to change signal DOA in BS.

IV. BASE STATION SIGNAL PROCESSING

Base station signal processing includes downlink signal processing for transmitter and uplink signal processing for receiver.

The grey boxes on the Fig. 6 indicate hardware units, which

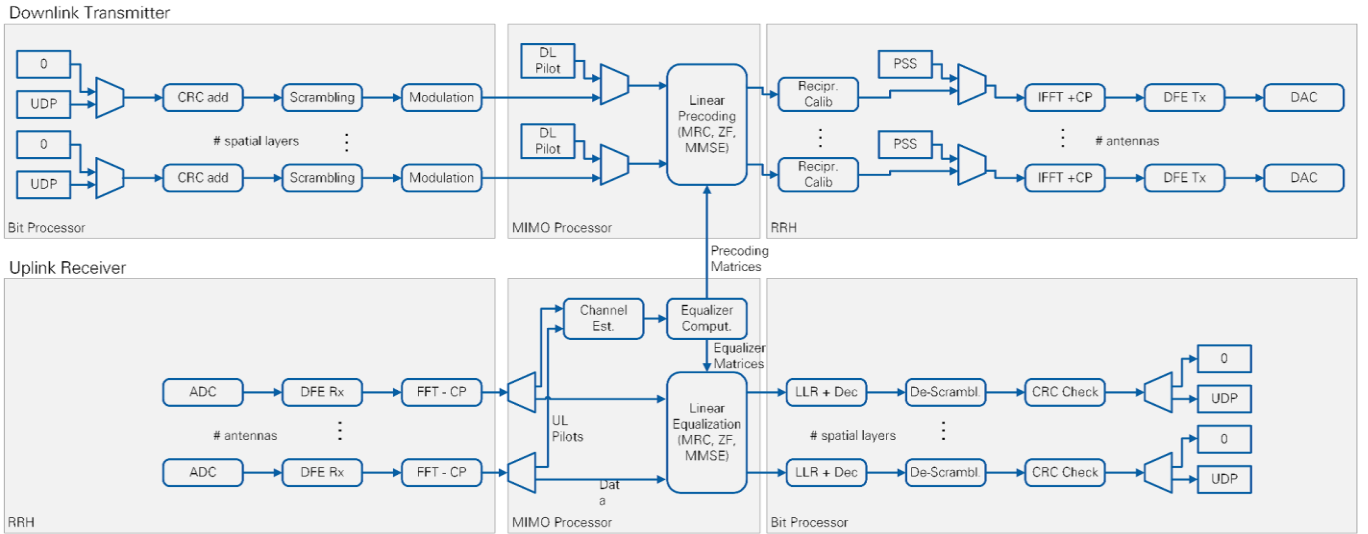


Fig. 6. Base station signal processing diagram

implement the respective signal processing functionality. The receiver signal processing include following main operations and blocks. At first, the signal at the output of each analog-to-digital converter is fed into the receive digital frontend block (DFE Rx). This block implements automatic DC offset correction and resampling from the native sampling frequency of the ADC to 30.72 MHz. The mobile stations are responsible for correcting carrier frequency offsets in their transmit signals and for adjusting their transmit timing such that the uplink signal arrives synchronous to the downlink frame timing. Hence, no further synchronization functionality is implemented at the base station receiver. Then the cyclic prefix is discarded and the signal is converted to frequency domain by 2048 size FFT (FFT-CP).

Uplink pilot signals are extracted from the frequency domain receive signal and fed into a channel estimation block. The Channel Estimation block computes channel transfer functions for all transmit-receive antenna combinations. All channel estimates are provided to the Equalizer Computation block. This block computes MIMO equalization matrices to be applied at each subcarrier by the Linear Equalization block in order to obtain estimates for the transmitted symbols. As mentioned, MIMO equalization matrices can be computed according to the maximum ratio combining, zero forcing, or minimum mean square error criterion. After equalization, the LLR + Dec block computes log likelihood ratios for all bits comprised in an equalized symbol, followed by a binary hard decision. De-Scrambling block applies an XOR operation with the scrambling sequence to the hard bits. The CRC Check block computes the CRC check sum based on the de-scrambled bits and the result is used to detect any hard decision errors in a sequence of hard bits. At the end, Header information is used to separate UDP payload and transmitted zeros.

The second chain of signal processing is intended for Transmitter. The base station transmitter generates signals for a configurable number of spatial layers. Data are transmitted uncoded, that is, without forward error correction.

Per spatial layer, either payload data are received at a UDP data interface, or zeros are transmitted. The CRC add block appends a frame check sequence (FCS) to the payload. In addition, it prepends a header containing the length of the UDP payload. Then the Scrambler block scrambles the binary input sequence. The scrambler ensures the transmission of a zero-mean random binary sequence, even if the input sequence comprised only zero values. The Modulation block maps groups of bits to M-QAM signals. Downlink pilot signals are inserted, depending on the frame schedule. Pilot position within a physical resource block depends on the layer. Pilots assigned to different layers are frequency orthogonal. Spatial layers are mapped to antennas in frequency domain by means of the Linear Precoding block. Precoding is applied to downlink pilot and data signals. Reciprocity calibration coefficients are applied in frequency domain per antenna by the Reciprocity Calibration block to compensate for the impact of non-reciprocal transmit and receive radio transceiver modules at the base station and to enable reciprocity based precoding. The Primary Synchronization Sequence is inserted, depending on the frame schedule. This sequence is not precoded and is transmitted from all antennas. The signal is converted to time domain per antenna by 2048 size FFT. A cyclic prefix is prepended.

Finally, the transmit digital frontend block DFE Tx resamples the signal from 30.72 MHz to the native sampling frequency of the digital-to-analog converters.

V. EXPERIMENTAL RESULTS

A. Channel Parameter Extraction

The experiments have been carried out indoors. In order to get channel parameters for different MS locations, BS and MS placed in a big room. Due to the absence of anechoic chamber, radio spectrum at the testbed dislocation place is carefully monitored and free spectrum windows were distinguished. Taking into account radio frequency spectrum freeness, the experiments have been carried out at a carrier frequency of 2.2 GHz. Signal wavelength could be calculated from the signal

frequency and equal to 13.6cm. For maximal precision, antenna spacing in both X and Y directions should be equal to $\lambda/2$ (6.8cm), inter element lower spacing is acceptable without rise of ambiguity, the higher element spacing will result in ambiguity of detected directions. We had used already mentioned antenna array configuration where distance among antennas in X direction is equal to 5cm and in Y direction to 4.5cm. For precise DOA estimation, minimum distance between BS and MS should meet far field conditions

$$r \geq \frac{2D^2}{\lambda} \approx 4.7 \text{ m}. \quad (15)$$

So distance between BS and MS kept 5 m. USRP R10s RF front ends connected to array elements through uncalibrated RF cables. This rises need for phase calibration and alignment. Phase calibration implemented by reciprocity calibration operation. More details on reciprocity calibration could be found in [12].

Channel parameter extraction is based on channel estimation, which is implemented in the frequency domain. It relies on frequency orthogonal pilots transmitted in uplink and downlink. The FFT size is 2048 and only 1200 subcarriers is used for information transmission and channel estimation, others serve as guard frequency interval. In order pilots for different layers to be frequency orthogonal, a length-100 subset of active subcarriers is selected for each spatial layer (or mobile station). A pilot corresponding to spatial layer 1 occupies the first subcarrier in each resource block (RB). A pilot corresponding to spatial layer 2 occupies the second subcarrier in each RB and so forth. There are 12 subcarriers at every RB.

The signal received in the uplink at all base station antennas, at a single subcarrier, originating from a single mobile station antenna can be modelled as

$$\mathbf{y}(t) = \mathbf{H}\mathbf{x}(t) + \mathbf{v} \quad (16)$$

where $\mathbf{x}(t)$ is transmit signal vector, $\mathbf{y}(t)$ is receive signal vector, \mathbf{H} is channel matrix in frequency domain and \mathbf{v} is white Gaussian noise vector.

The channels complex coefficients matrix \mathbf{H} for pilot subcarrier, at specific time is estimated according to (17)

$$\hat{\mathbf{H}} = \mathbf{y} \cdot \frac{\mathbf{x}^H}{|\mathbf{x}|^2} = \frac{\mathbf{x} \cdot \mathbf{x}^H}{|\mathbf{x}|^2} + \frac{\mathbf{v} \cdot \mathbf{x}^H}{|\mathbf{x}|^2}. \quad (17)$$

The first term in (17) is sample covariation matrix for each subcarrier, the second term is noise component. Equation (17) is similar to (14).

The channels estimates acquired at channel estimation block are transferred from FPGA to the Host through DMA first-in first-out memory buffers (FIFOs). In the Host they are further processed according to the proposed algorithm to obtain DOA estimates for 2D antenna array. A chunk of real channel estimates is saved into .txt file and available in open access for further experimentation [13].

B. DOA Estimation Algorithm

The goal of the beamforming DOA estimation techniques is

low computational complexity compared to parametric approaches. Usually, in order to simplify the analysis and rise positioning precision, a uniform linear array with inter-element spacing of half wavelength of the impinging signal frequency is assumed. This kind beamforming DoA estimation algorithm implementation for the uniform linear arrays could be found in many sources. We have implemented algorithm for 2D planar array with arbitrary inter element spacing. Channel state information acquired by BS (phase and amplitude of certain OFDM subcarrier) is used as initial data for calculation.

The total field pattern from an array could be found by multiplying the array element factor (the pattern produced by a single element) by the array factor [5]. The array factor represents the response of an array of isotropic elements. Those allow us to treat the element and the array separately.

$$\mathbf{AF}(\theta, \varphi) = \mathbf{AF}_{Element}(\theta, \varphi) \cdot \mathbf{AF}_{Array}(\theta, \varphi) \quad (18)$$

Antenna factor of array element in both H and E planes could be found in VERT 2450 specification [14]. Using interpolation we obtained array element pattern 3D model. It could be found in sample program [15].

For 2D planar array with elements arranged uniformly along a rectangular grid in the xy-plane, with an element spacing d_x in the x-direction and an element spacing d_y in the y-direction, it is useful to use two indices to refer to the elements: a row index and a column index. Grid indices in the x and y direction are denoted as m and n respectively. The position vector of the mnth element is given by

$$\vec{r}_{mn} = x_{mn}\vec{x} + y_{mn}\vec{y} + z_{mn}\vec{z}. \quad (19)$$

We have spacings indicated and the array starts at the coordinate system origin, so we can rewrite position vector expression as

$$\vec{r}_{mn} = md_x\vec{x} + nd_y\vec{y} \quad (20)$$

where in our case $m=\{1, 2, 3, \dots, 8\}$, $n=\{1, 2\}$.

The array factor expression is then written as follows, where we have split the summation into two summations along each dimension:

$$\begin{aligned} \mathbf{AF}_{Array}(\theta, \varphi) &= \sum_{n=1}^2 \sum_{m=1}^8 I_{mn} e^{jk(\vec{r} \cdot \vec{r}_{mn})} = \\ &= \sum_{n=1}^2 \sum_{m=1}^8 I_{mn} e^{jk(md_x \sin \theta \cos \varphi + nd_y \sin \theta \sin \varphi)} \end{aligned} \quad (21)$$

where I_{mn} denotes the excitation amplitude of the mnth element of the array, and is a real number, and \vec{r} is a unit vector pointing in the direction of interest,

$$\vec{r} = \sin \theta \cos \varphi \vec{x} + \sin \theta \sin \varphi \vec{y} + \cos \theta \vec{z}. \quad (22)$$

Inserting (21), (18), and (17) into (13) and taking into account that antenna factors are normalized, we obtain 2D pseudospectrum calculation equation:

$$\begin{aligned}
\mathbf{P}(\theta, \varphi) &= \mathbf{A}\mathbf{F}(\theta, \varphi) \cdot \mathbf{A}\mathbf{F}(\theta, \varphi)^H \cdot \hat{\mathbf{H}} = \\
&= \left(\mathbf{A}\mathbf{F}_{Element}(\theta, \varphi) \sum_{n=1}^2 \sum_{m=1}^8 I_{mn} e^{jk(md_x \sin \theta \cos \varphi + nd_y \sin \theta \sin \varphi)} \right) \\
&\cdot \left(\mathbf{A}\mathbf{F}_{Element}(\theta, \varphi) \sum_{n=1}^2 \sum_{m=1}^8 I_{mn} e^{jk(md_x \sin \theta \cos \varphi + nd_y \sin \theta \sin \varphi)} \right)^H \\
&\cdot \hat{\mathbf{H}}
\end{aligned}$$

The peak in the 2D pseudospectrum represents the estimated DOA of the incoming signal. The 2D pseudospectrum is symmetrical against XY plane and in order to solve ambiguity for peak search only $\varphi = (0^\circ; 180^\circ], \theta = (0^\circ; 180^\circ]$ range is used (BS front direction). Calculation resolution is set to 1° , and could be modified in software.

C. DOA Estimation Results

Experimental DOA estimation results acquired by using channel state information for several angles of impinging signal. Taking into account radiation patterns of array elements and MS antenna, we avoid placing MS below and above BS. In case of vertical arrangement of array elements, estimation precision degrades severely on these directions. Estimation results for one of the cases with actual azimuth angle of impinging signal 54° is depicted in Fig. 7.

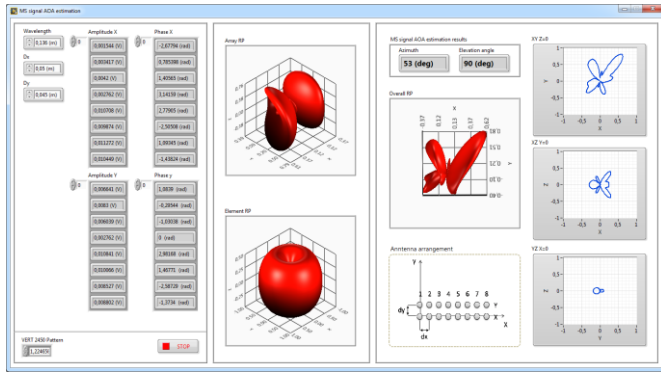


Fig. 7. Front panel of DOA estimation program.

Estimated value of elevation angle is constant during experiment and equal to actual value 90° (BS and MS is placed on the tables having the same height). Estimated value of azimuth angle is trends to fluctuate around actual value with deviation $\pm 1^\circ$. The estimation is also affected by reflections from walls and thus estimation precision of 1° is a good result.

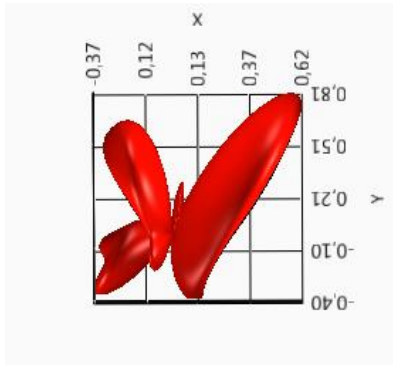
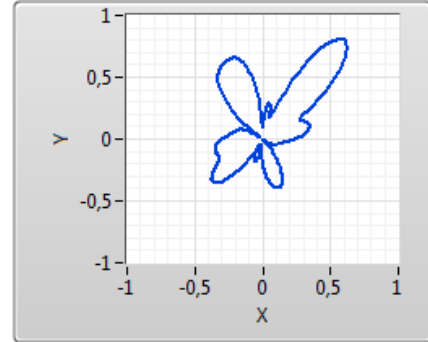
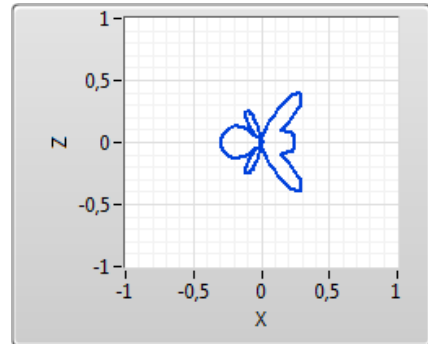


Fig. 8. Estimated 3D pseudospectrum.

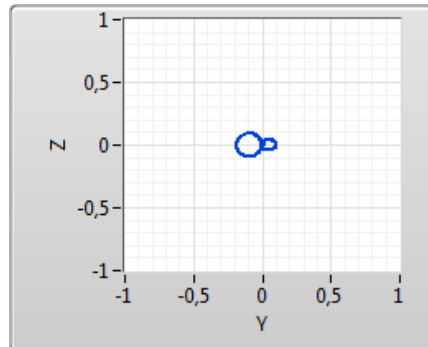
The estimated 3D pseudospectrum is presented in Fig. 8 and sections of 3D pseudospectrum in XY, XZ, YZ planes are presented in Fig. 9.



(a) Section in XY plane



(b) Section in XZ plane



(c) Section in YZ plane

Fig. 9. Sections of 3D pseudospectrum.

VI. CONCLUSION

In this work, computationally light extension of classical DOA estimation method is implemented on a MIMO prototyping platform. Experimental results in multipath propagation environment show that the system is able to estimate the directions of MS with quite good precision ($\pm 1^\circ$). The software exploits the key features of MIMO and OFDM. The inter layer and inter antenna frequency orthogonally of pilot subcarriers allows to get channel parameters for all of them separately and simultaneously estimate signal DOAs of all MSs under service. During further research, DOAs for all subcarriers could be calculated independently and averaging of calculated

angles will be utilized to increase DOA estimation precision even in low SNR scenarios. Additional usage of Time Of Arrival (TOA), Round Trip Time Of Arrival (RTTOA) parameters in single BS scenario and Differential Time Of Arrival (DTOA) parameter in multi BS scenario will allow to estimate distance between BS and MS. This in turn opens possibility for positioning and position tracking.

The system and the software are flexible for further modifications or expansions by modifying the design software. The open source software for further research is available on GitHub.

ACKNOWLEDGMENT

The authors appreciate the valuable help from K. Vardanyan and H. Hovsepyan, and would like to thank to NI Armenia and ISTC for all the support provided allowing to obtain the results of this article.

REFERENCES

- [1] A. Osseiran *et al.*, "Scenarios for 5G mobile and wireless communications: The vision of the METIS project," *IEEE Commun. Mag.*, vol. 52, no. 5, pp. 26–35, May. 2014., doi:10.1109/mcom.2014.6815890
- [2] F. Perez-Fontan, B. Sanmartin, A. Steingass, A. Lehner, J. Selva, E. Kubista and B. Arbesser-Rastburg, "A high resolution model for the satellite-to-indoor channel," in *Proc. Position location and navigation symposium (PLANS), 2004*, pp. 674–683, doi:10.1109/plans.2004.1309059.
- [3] K. V. Rangarao and S. Venkatunarasimhan, "Gold-MUSIC: A variation on MUSIC to accurately determine peaks of the spectrum," *IEEE Trans. On Antennas and Prop. Mag.*, vol. 61, no. 4, pp. 2263–2268, April. 2013. doi:10.1109/tap.2012.2232893
- [4] I. Ziskind and M. Wax "Maximum likelihood localization of multiple sources by alternating projection," *IEEE Trans. On Acoustics, Speech and Sig. Proc.*, vol. 36, no. 10, pp. 1553–1560, Oct. 1988., doi:10.1109/29.7543
- [5] F. B. Gross, "Smart antennas with MATLAB," 2nd ed., New York, NY, USA: McGraw-Hill, 2015, pp. 208–250.
- [6] D. Gesbert, M. Kountouris, R. W. Heath, C. Chae and T. Salzer, "Shifting the MIMO paradigm," *IEEE Sig. Proc. Mag.*, vol. 24, no. 5, pp. 36–46, Oct. 2007. doi:10.1109/msp.2007.904815
- [7] M. Abusultan, S. Harkness, B. J. LaMeres and Y. Huang, "FPGA implementation of a Bartlett direction of arrival algorithm for a 5.8 GHz circular antenna array," presented at the *IEEE Aerospace Conference, Big Sky, MT, USA, March. 6-13, 2010*. doi:10.1109/aero.2010.5446970
- [8] P. Boonyanant and S. Tan-a-ram, "FPGA implementation of a subspace tracker based on a recursive unitary ESPRIT algorithm," in *Proc. IEEE Region 10 Conference (TENCON), 2004*, pp. 547–550., doi:10.1109/tenc on.2004.1414478
- [9] M. Arenas, A. Podhorski, S. Arrizabalaga, J. Goya, B. Sedano and J. Mendizabal "Implementation and validation of an angle of arrival (AOA) determination system," presented at the *Conference on Design of Circuits and Integrated Systems (DCIS), Estoril, Portugal, Nov. 25-27, 2015*. doi:10.1109/dcis.2015.7388579
- [10] H. Krim and M. Viberg, "Two decades of array signal processing research: The parametric approach," *IEEE Sig. Process. Mag.*, vol. 13, no. 4, pp. 67–94, July. 1996. doi:10.1109/79.526899
- [11] National Instruments, (2017, Aug), 376638B-01, MIMO Prototyping System. Available: <http://www.ni.com/pdf/manuals/376638b.pdf>
- [12] C. Shepard, H. Yu, N. Anand, E. Li, T. Marzetta, R. Yang, and L. Zhong, "Argos: Practical many-antenna base stations," in *Proc. 18th Annual International Conference on Mobile Computing and Networking, 2012*, pp. 53–64. doi:10.1145/2348543.2348553
- [13] NPUA, (2018, Sep.), Measured channel state information. Available: [https://github.com/LevonGR/DOA-Estimator/blob/master/Channel%20state%20information%20\(Static%20MS%20position%20tetta=90%20fi=54\)%20vertical%20antennas.txt](https://github.com/LevonGR/DOA-Estimator/blob/master/Channel%20state%20information%20(Static%20MS%20position%20tetta=90%20fi=54)%20vertical%20antennas.txt)
- [14] Ettus Research, (2017, Aug), Vert2450, Vert 2450 Datasheet. Available: https://kb.ettus.com/images/9/9e/ettus_research_vert2450_datasheet.pdf
- [15] NPUA, (2018, Sep), MIMO OFDM Host DOA estimator. Available: <https://github.com/LevonGR/DOA-Estimator>



Levon N. Grigoryan received the B.S. and M.S. degrees in radio engineering from the National Polytechnic University of Armenia, Yerevan, in 2014 and 2016 respectively. He is currently pursuing the Ph.D. degree in telecommunications engineering at National Polytechnic University of Armenia, Yerevan, Armenia. Since 2016, he has been a researcher with the 5G Research Group at Institute of IT and Electronics, NPUA, Yerevan, Armenia. His research interests include the signal processing and mobile communications.



Martin Ts. Aivazyan received the M.S. degree in radio engineering from Institute of Radio Physics and Electronics of Armenian academy of Science, Yerevan, Armenia, in 1979 and the Ph.D. degree in Radio electronics from Institute of Radiotechnics and Electronics of academy of Science, Moscow, Russia, in 1982. From 1982 to 1990, he was a senior scientific worker with the Institute of Radio Physics and Electronics of Armenian academy of Science, Yerevan, Armenia. Currently he is an Associate Professor and Head of 5G Research Group with the Institute of IT and Electronics, National Polytechnic University of Armenia, Yerevan, Armenia. His research interests include mmWave communications, RF component design and mobile communications.



Arshak S. Babayan received the B.S. degrees in radio engineering from the National Polytechnic University of Armenia, Yerevan, in 2016 and the M.S. degree in information systems and technology from Moscow Technological University (MIREA), Moscow, Russia, in 2018. He is currently pursuing the Ph.D. degree in telecommunications engineering at National Polytechnic University of Armenia, Yerevan, Armenia. Since 2018, he has been a researcher with the 5G Research Group at Institute of IT and Electronics, NPUA, Yerevan, Armenia. His research interests include the internet of things and mobile communications.